Spatial Frequency Performance of SPRITE Detectors

Glenn D. Boreman
University of Central Florida
CREOL/Electrical Engineering Department
Orlando, Florida 32816

Allen E. Plogstedt
McDonnell Douglas Astronautics Company
701 Columbia Blvd.
Titusville, Florida 32780

ABSTRACT

SPRITE (Signal PRocessing In The Element) detectors are analyzed in terms of their main spatial frequency dependent parameters of modulation transfer function and number of equivalent elements.

1. INTRODUCTION

SPRITE detectors (refs. 1-10) are photoconductive structures which exploit the finite carrier drift velocity in a semiconductor material to achieve an enhancement in signal to noise ratio, by means of time-delay-and-integration (TDI). TDI is a technique which facilitates an increased "dwell time" of the detector on each element of the scene. This increased dwell time is equivalent to signal averaging, and hence the signal grows coherently in proportion to the observation time and the noise grows incoherently in proportion to the square root of the observation time. This is implemented by physically scanning the infrared scene past the SPRITE detector at the same velocity as the photogenerated carriers drift under the applied electric field. The signal to noise enhancement is achieved at the expense of spatial resolution, because as the carriers drift in the semiconductor, they also undergo diffusion, which makes the impulse response of the detector larger with increased dwell time.

The basic structure of a SPRITE is seen below in Fig.1. The image data is available as the voltage across the read-out region, which is modified by the carrier concentration which moves past the read-out. Fig.2 illustrates two design parameters which are often useful: the length of the SPRITE element and the shape of the read-out region.

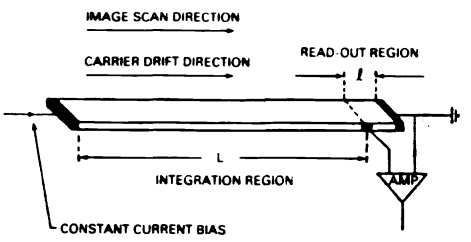

Fig.1. Basic structure of the SPRITE.

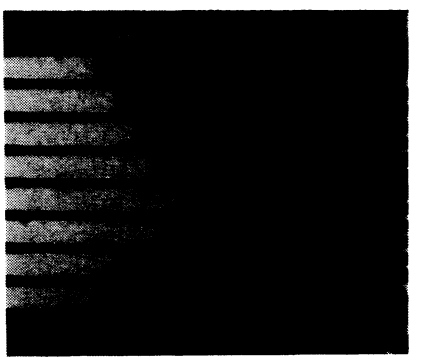

Fig.2. SPRITE array of variable bar length, with a tapered read-out region.

2. MODULATION TRANSFER FUNCTION

The modulation transfer function (MTF) of the SPRITE detector may be obtained from the Fourier transform of the impulse response of the device. Our analysis concentrates on two major components of the MTF, arising from carrier diffusion and recombination, and from the shape of the read-out region.

2.1 MTF due to carrier diffusion and recombination

Following the procedure used by Day and Shepherd (Ref.3), the component of MTF due to carrier diffusion and recombination may be found using the following impulse response for the semiconductor, which accounts for both effects:

$$G(x,t) = \frac{1}{2\sqrt{\pi D t}} \exp - \left[\frac{(x - \mu E t)^2}{4 D t} + \frac{t}{\tau} \right] . \qquad (1)$$

In the above equation, x is spatial position, t is time (assuming that the charge is generated at x=0 and t=0), D is the diffusion constant of the material, τ is the carrier lifetime, μ is the carrier mobility and E is the electric field impressed across the length of the SPRITE. The diffusion length of carriers in the material is $L_D = \sqrt{D \tau}$. The mean carrier drift length before recombination is $\mu E \tau$. The qualitative behavior of this impulse response may be seen in Fig.3, where G is plotted versus x/L_D at various instants in time (this figure was adapted from Ref.3, and is plotted for $\mu E \tau = 6\ L_D$).

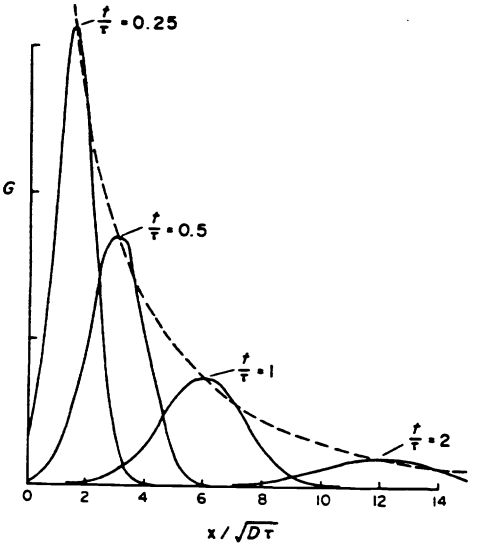

Fig.3. Impulse response of the detector material, as a function of time and position.

The MTF of the SPRITE due to carrier diffusion and recombination is found (Ref.9) by performing the Fourier transform of this impulse response in both the space and time domains, taking into account the finite length of the SPRITE element. Once the transform of this impulse reponse is normalized to unity at low spatial frequency, the following expression for MTF obtains:

$$MTF(\xi,L) = \frac{\frac{1}{(L_D^2\,\xi^2 + 1)}\left[1 - \exp\left[-(L_D^2\,\xi^2 + 1)\,\frac{L}{\mu E\tau}\right]\right]}{1 - \exp(-L/\mu E\tau)} \qquad (2)$$

where ξ is spatial frequency (radians/distance) and L is the length of the SPRITE element. The MTF is shown in Fig.4, plotted as a function of normalized spatial frequency (ξL_D), with normalized bar length ($L/(\mu E\tau)$) as a parameter.

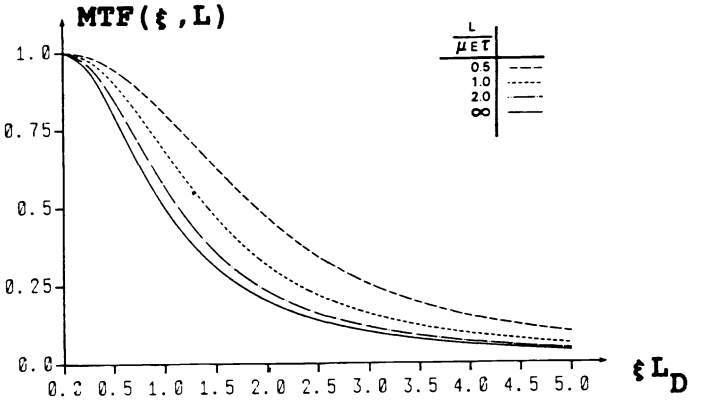

Fig.4. MTF of the SPRITE as a function of spatial frequency and element length.

We note that the MTF is increased by decreasing the length of the SPRITE element. The charge packet undergoes diffusion as it travels down the element. If the bar is too short for the attainment of a steady state spot size due to diffusion, then the smaller size of the charge packet gives a better spatial resolution for the SPRITE. Another feature of Fig.4 is that a SPRITE fabricated from a semiconductor material with a small diffusion length L_D (generally having a small carrier lifetime τ) will have a higher MTF than a SPRITE using a material with a longer diffusion length.

It is of interest, from the point of view of comparision with previously published work, that in the limit of long bar length ($L>>\mu E\tau$), Eq.2 yields the usual MTF expression:

$$MTF(\xi,L) = \frac{1}{(L_D^2\,\xi^2 + 1)} \qquad (3)$$

A gain in MTF naturally comes at the expense of signal to noise ratio, since a short element (or a material with a small carrier lifetime) has a shorter dwell time on a particular scene feature. We will consider the engineering tradeoff of MTF versus signal to noise ratio in section 3.

2.2 MTF due to the read-out shape

In this section, we treat the read-out region separately from the rest of the SPRITE, for purposes of an MTF analysis. We obtain

an expression for the MTF of the read-out, which can be multiplied with the MTF obtained in the previous section, to give an overall device MTF. As seen in Fig.2, the readout region of the SPRITE can have a tapered shape. This is a technique which is used to enhance the MTF of the SPRITE. One interpretation of the mechanism of such a structure is that the taper reduces the dispersion of carrier transit times through the read-out (Ref.6). We present an easy-to-use, alternative model of these structures which appears to have a better agreement with experimental results.

The read-out region of the SPRITE is photosensitive, and as such, is a detector element which is scanned over the image presented to the SPRITE. Our model for MTF of these structures begins with the fact that a detector of finite size performs a spatial averaging of the flux which falls on it. This spatial averaging process has the effect of filtering the image data in the Fourier domain. The process of scanning a detector past a spatially varying irradiance may be cast (Ref.10) as a convolution between the irradiance i(x,y) and the detector spatial responsivity profile d(x,y), which is taken for convenience to be a "one-zero" function, i.e., either unity inside or zero outside. Assuming for the moment that the detector is free to scan in both the x and y directions, we may write the following expression for the output of the detector as a function of scan position, $r(x_s,y_s)$:

$$r(x_s,y_s) = i(x,y) \;**\; d(x,y) \;, \qquad (4)$$

where ** indicates a two-dimensional convolution. For a line-scanned detector such as the SPRITE, Eq.4 needs to be modified to give the response of the detector along one particular horizontal scan line, here taken to be the line $y_s=0$:

$$r(x_s,0) = [i(x,y) \;**\; d(x,y)] \times [1(x_s)\; \delta(y_s)] \;. \qquad (5)$$

We can obtain $R(\xi)$, the 1-D Fourier transform of $r(x_s,0)$ by means of the convolution theorem:

$$R(\xi) = \mathcal{F}\{r(x_s,0)\} = [I(\xi,\eta) \times D(\xi,\eta)] \;**\; [\delta(\xi)\; 1(\eta)] \;, \qquad (6)$$

where $\mathcal{F}$ is the 1-D Fourier transform operator, ξ is the along-scan spatial frequency variable and η is the perpendicular-to-scan spatial frequency variable. The convolution in the η direction produces a constant which normalizes out under the usual definition of MTF, so that the MTF for the read-out structure (in the along-scan direction) is written as

$$MTF(\xi) = |D(\xi,0)/D(0,0)| \;. \qquad (7)$$

We can now compare the MTF of two typical read-out structures: one is rectangular of length X and height Y; one is exponentially-tapered; having the same total length X, but now tapered along the x direction.

Using Eq.7 for the rectangular structure of width X, calculation of the MTF yields simply

$$MTF(\xi) = |\mathrm{sinc}(X\xi)| \ . \qquad (8)$$

The photosite responsivity function d(x,y) was separable, so that $D(\xi,0)$ could be calculated simply as $\mathcal{F}\{d(x,0)\}$.

The geometry for the tapered readout is shown in Fig.5. The height of d(x,y) in the y direction depends upon the x coordinate. In order to calculate the MTF for this structure, we again need to find an expression for $D(\xi,0)$. However, in this case, we have a non-separable function for d(x,y), i.e., d(x,y) cannot be expressed simply as a function of x multiplied by a function of y. This implies $D(\xi,0) \neq \mathcal{F}\{d(x,0)\}$, i.e., that the ξ profile of the 2-D transform of the photosite responsivity is not simply the 1-D transform of the x-profile of that responsivity. The non-separability of d(x,y) in this case implies that the y-profile of the photosite response function comes explicitly into the calculation of the MTF in the ξ direction.

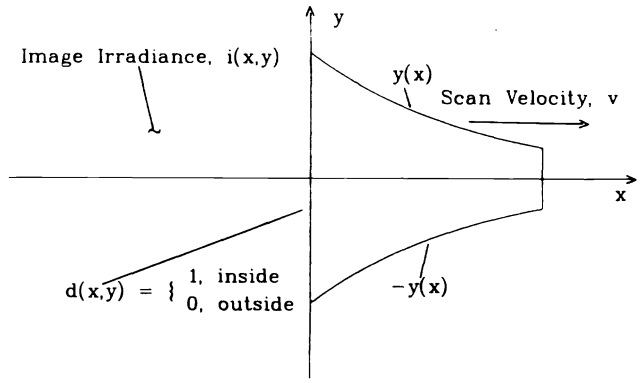

Fig.5. Geometry for the tapered read-out structure.

We proceed as follows:

$$D(\xi,\eta) = \int_{-\infty}^{\infty}\int d(x,y)\ \exp(-j2\pi\xi x)\ \exp(-j2\pi\eta y)\ dx\ dy \ . \qquad (9)$$

Since d(x,y) is a "one-zero" function, we may write Eq.9 as

$$D(\xi,\eta) = \int_{-\infty}^{\infty} \exp(-j2\pi\xi x) \int_{-y(x)}^{y(x)} \exp(-j2\pi\eta y)\ dy\ dx \ . \qquad (10)$$

Along the η=0 profile which is of interest for MTF(ξ), Eq.10 becomes

$$D(\xi,0) = \int_{\infty}^{\infty} \exp(-j2\pi\xi x) \int_{-y(x)}^{y(x)} dy\ dx = \int_{\infty}^{\infty} \exp(-j2\pi\xi x)\ 2y(x)\ dx = 2Y(\xi) \ . \qquad (11)$$

Applying Eq.7, we obtain

$$MTF(\xi) = |Y(\xi)/Y(0)| \ . \qquad (12)$$

For the tapered read-out, the profile y(x) of the photosite responsivity is of the form

$$y(x) = \text{rect}\left[\frac{x - X/2}{X}\right] \exp(-\alpha x), \qquad (13)$$

where α is the tapering coefficient. Thus, because of the convolution theorem, the MTF of the tapered read-out will be wider than the MTF of the rectangular readout of the same length.

$$MTF(\xi) \propto \mathcal{F}\left[\text{rect}\left[\frac{x - X/2}{X}\right]\exp(-\alpha x)\right]$$

$$= \mathcal{F}\left[\text{rect}\left[\frac{x-X/2}{X}\right]\right] * \mathcal{F}\{\exp(-\alpha x)\} \ . \qquad (14)$$

In Fig.6, we present a comparison of MTF for two typical read-out structures: one is rectangular with dimensions 50μm long in the x direction and 35μm wide in the y direction; the other is exponentially-tapered, also 50μm long in the x direction, and 62.5μm wide at the wide end and 15μm wide at the narrow end (α = 0.0285). The tapered read-out is seen to have a better MTF than the rectangular read-out. A comparison of these curves with measured data is made in Ref.10. A good agreement is found, with the advantage that the MTF for a particular read-out geometry is easily calculated from the geometry of the structure.

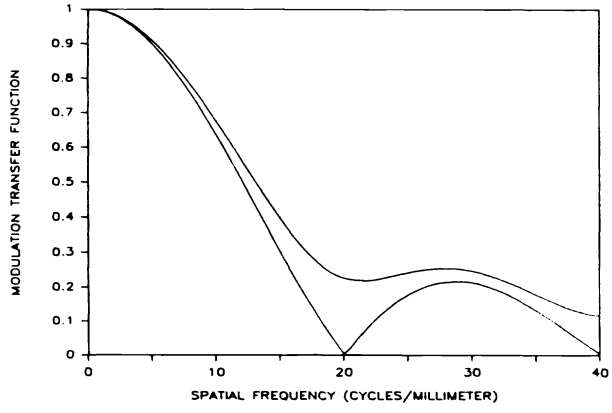

Fig.6. Comparison of MTF of rectangular (lower curve) and tapered (upper curve) read-out structures.

As stated at the beginning of this section, the read-out MTF seen above can be multiplied by the MTF due to carrier diffusion and recombination to obtain the MTF for the entire SPRITE device.

3. NUMBER OF EQUIVALENT ELEMENTS

In section 2.1, it was found that the MTF of the SPRITE is better for shorter element lengths. This MTF enhancement comes at the expense of signal to noise ratio, since a short element has a shorter dwell time on a particular scene feature. We now consider the dependence of signal to noise ratio on bar length and spatial frequency by the figure of merit N_{eq}, the number of equivalent elements.

N_{eq} is the number of discrete detector elements in TDI which would produce the same signal to noise ratio enhancement as the SPRITE bar. Recall that in the classical TDI situation of n detectors scanned serially, the signal strength grows in proportion to n, and the noise grows as the root of n, since the signal is correlated and the noise is uncorrelated from element to element. Thus, for the classical TDI case, the signal to noise ratio grows as $\sqrt{n}$. We can define the number of equivalent elements on the same basis, that of signal strength. Thus, N_{eq} is the ratio of the signal strength which would be obtained by a SPRITE element of length L to the signal strength which would be obtained by a SPRITE element of length ℓ of the read-out alone. By analogy with the classical TDI case, the signal to noise enhancement obtained with the SPRITE may be interpreted as $\sqrt{N_{eq}}$. The signal strength as a function of element length and spatial frequency is obtained (Ref.9) via a Fourier transform of the impulse response given in Eq.1, but without the normalization to unity at zero spatial frequency which was necessary for the MTF calculated in Eq.2. Thus, the expression for N_{eq} becomes

$$N_{eq}(\xi;L) = \frac{1 - \exp\left[- (L_D^2 \xi^2 + 1) \frac{L}{\mu E \tau} \right]}{1 - \exp\left[-(L_D^2 \xi^2 + 1) \frac{\ell}{\mu E \tau} \right]} \qquad (15)$$

which is shown in Fig.7. N_{eq} is plotted as a function of normalized bar length, with normalized spatial frequency as a parameter. For the plots, a readout length of 0.1 times the mean drift length before recombination was assumed. There are several features of the plots worth noting: Increasing bar length gives a larger value of N_{eq}, but for any given spatial frequency, there is a particular bar length for which the majority of signal to noise enhancement has been obtained. For low spatial frequencies, it takes a longer element length to obtain the majority of the available signal to noise enhancement. There is more signal to noise enhancement available at low spatial frequencies. The interpretation can be made that the carrier diffusion limits the available integration of signal at high spatial frequencies.

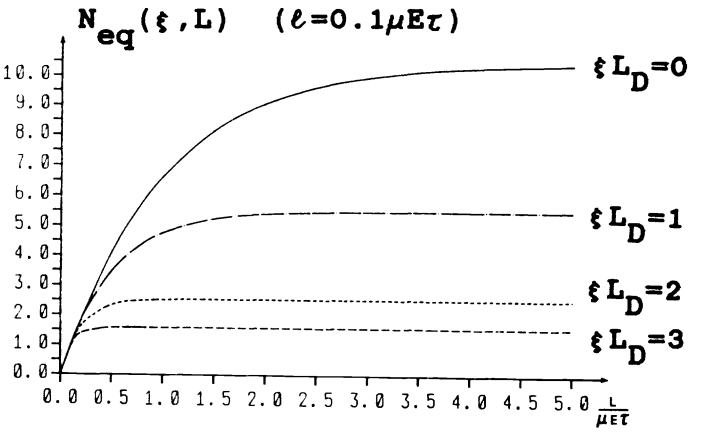

Fig.7. N_{eq} as a function of SPRITE length and spatial frequency.

An approximation to Eq.15 under a specific combination of limits is also of interest. At low spatial frequencies ($\xi \approx 0$), and for a SPRITE having an element of length L which is long and a read-out dimension ℓ which is short, both compared to the mean drift length before recombination ($L >> \mu E\tau >> \ell$), Eq.14 has the following limiting form:

$$N_{eq} \approx \mu E\tau/\ell \ , \qquad (16)$$

which is the mean drift length before recombination divided by the read-out length.

4. SYSTEM OPTIMIZATION

The effect of SPRITE element length has been seen to have competing effects on two figures of merit which are important for thermal imager performance. As the element is shortened, the MTF is enhanced, but at the expense of signal to noise ratio. An engineering trade-off is necessary for the system designer to decide on the proper element length. To illustrate the optimization procedure, a system-wide figure of merit may be taken to be the product of MTF and $\sqrt{N_{eq}}$. Both components of this figure of merit are functions of spatial frequency and bar length. Plots of this merit function (excluding the effect of read-out MTF) are shown in Fig.8. An appropriate optimization for element length would involve a maximization of the area under the merit function curve. The decicing factor in the choice of element length will then be the range of spatial frequencies over which the system is required to operate. It can be seen from Fig.8 that a system operating at predominantly low spatial frequencies would benefit from a long SPRITE element, while a system operating at predominantly high spatial frequencies would benefit from a short SPRITE element.

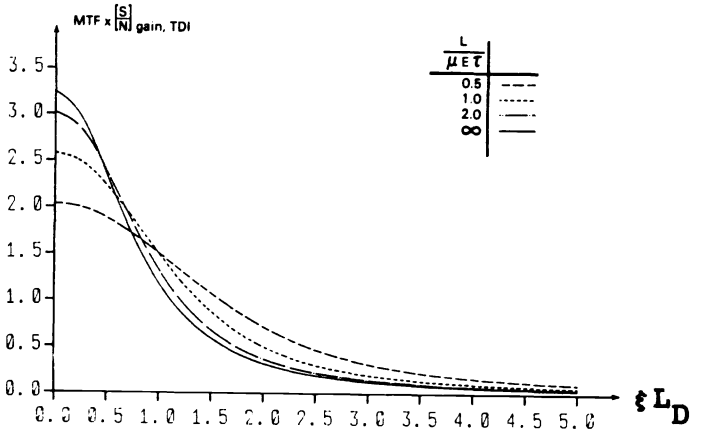

Fig.8. System merit function (MTF × $\sqrt{N_{eq}}$) as a function of spatial frequency and SPRITE element length.

5. CONCLUSIONS

Expressions have been presented for the MTF of SPRITE detectors due to carrier diffusion and recombination, and due to the shape of the read-out region. MTF has been seen to depend on the length of the SPRITE element. The enhancement of signal to noise ratio also depends upon the element length, and can be expressed in terms of the number of equivalent elements. A figure of merit has been presented which allows the optimization of performance, as a function of the length of the SPRITE element.

6. REFERENCES

1. C.T. Elliott, "New Detector for Thermal Imaging Systems", *Electronics Letters* 17, 312 (1981).
2. C.T. Elliott, D. Day, and D.J. Wilson, "An Integrating Detector for Serial Scan Thermal Imaging", *IR Physics* 22, 31 (1982).
3. D.J. Day and T.J. Shepherd, "Transport in Semiconductors-I", *Solid State Electronics* 25, 707 (1982).
4. T.J. Shepherd and D.J. Day, "Transport in Semiconductors-II", *Solid State Electronics* 25, 713 (1982).
5. A. Blackburn, M.V. Blackman, D.E. Charlton, W.A.E. Dunn, M.D. Kenner, K.J. Oliver, J. Wotherspoon, "The Practical Realization and Performance of SPRITE Detectors", *Infrared Physics* 22, 57 (1982).
6. T. Ashley, C.T. Elliott, A.M. White, J. Wotherspoon, and M.D. Johns, "Optimization of Spatial Resolution in SPRITE Detectors", *Infrared Physics* 24, 25 (1984).
7. G.V. Poropat, "The Effect of Bias Voltage on SPRITE Detector Modulation Transfer Function (MTF)", *Infrared Physics* 26, 9 (1985).
8. A.B. Dean, P.N.J. Dennis, C.T. Elliot, D. Hibbert, J.T.M. Wotherspoon, "The Serial Addition of SPRITE Infrared Detectors", *Infrared Physics* 28, 271 (1988).
9. G.D. Boreman and A.E. Plogstedt, "Modulation Transfer Function and Number of Equivalent Elements for SPRITE Detectors", *Applied Optics* 27, 4331 (1988).
10. G.D. Boreman and A.E. Plogstedt, "Spatial Filtering by a Line-Scanned Nonrectangular Detector: Application to SPRITE Readout MTF", *Applied Optics* 28, 1165 (1989).